Computers & Structures Vol. 41, No. 4, pp. 687–707, 1991
Printed in Great Britain.

0045-7949/91 $3.00 + 0.00
Pergamon Press plc

PROBABILISTIC MULTI-OBJECTIVE OPTIMAL DESIGN OF SEISMIC-RESISTANT BRACED STEEL FRAMES USING ARMA MODELS

I. TAKEWAKI,† J. P. CONTE,‡ S. A. MAHIN and K. S. PISTER
Department of Civil Engineering, University of California, Berkeley, CA 94720, U.S.A.

(*Received* 11 *September* 1990)

Abstract—The objective of this paper is to develop a probabilistic multi-objective optimal design method for concentrically braced steel frames, including the design earthquake via a dynamic ARMA (Auto-Regressive Moving Average) model. The features of this design method are: (i) to make it possible to incorporate inherent uncertain features of design earthquakes into the design process itself through the dynamic ARMA model, (ii) to provide a simplified design formula for a preliminary design of concentrically braced steel frames based upon the concept of decomposed stiffness design, and (iii) to facilitate the formulation of a new probabilistic multi-objective optimal design problem aimed at finding the design with the minimum level of designer's dissatisfaction. In this optimal design problem, constraints and objectives are handled in a unified manner after a feasible design is obtained. Two design examples are presented to demonstrate the validity of this design method. Finally, the generality and practicality of the design method are assessed.

1. INTRODUCTION

At present, it is generally agreed that while the state of analysis of the response of given structures to deterministic seismic loading is well established, the state of design of earthquake-resistant structures is not at the level of advancement comparable to that of the state of analysis. The earthquake-resistant design of building structures using optimization concepts is one of the most challenging and complicated problems facing structural engineers (see [1]). One of the difficulties arises from the insufficient development of reliable and efficient optimization algorithms or the diversity of formulation of optimization problems and definition of optimality, which seem to depend largely on the subjectivity or intuition of each structural engineer.

Several techniques have been proposed for generating a population of design earthquakes. Most existing models for the analysis and simulation of earthquake ground motions are defined in the continuous time domain. On the other hand, recent interest has been increasingly focused on models formulated explicitly in discrete time. A dynamic ARMA (Auto-Regressive Moving Average) (2, 1) model is adopted in this paper. One of the principal advantages of using the dynamic ARMA model is to be able to gain insight into the inherent variability of seismic structural response as propagated from the inherent source of uncertainty attached to the ground motion time history. The input motion model for stochastic earthquake response analysis is extremely important due to the fact that the source of uncertainty of the structural response process results mainly from the earthquake input uncertainty (for example, see [2]).

Among several existing algorithms for decision making in engineering design environments, the mathematical programming technique appears to be the most general method to solve constrained optimum design problems. Every currently available mathematical programming algorithm requires the specification of an initial design. It is well known that this initial design significantly influences the final solution and that poor judgment at the preliminary design stage often results in a greater number of iteration cycles for design improvement. In developing a new design method, it is of great importance to balance the reliability of the method and the amount of the computational task required for implementing the design procedure.

It is well known that the interstory drift of a building frame under seismic loading can be reduced significantly by using bracing systems (for example, see [3]). In the case where the bracing system sustains a fairly large part of the story shear, the nonlinear behavior of the braced frame is influenced by the nonlinear restoring force characteristics of the bracing system. It is therefore necessary and desirable to clarify the nonlinear characteristics of the bracing system and to control the ratio of the bracing stiffness to the total story stiffness.

The objectives of this paper are (i) to present a simplified stiffness-oriented static design method, called 'decomposed stiffness design method', for concentrically braced steel frames, (ii) to develop a

† Present address: Department of Architecture, Kyoto University, Sakyo, Kyoto 606, Japan.
‡ Present address: Department of Civil Engineering, Rice University, Houston, TX 77251, U.S.A.

dynamic stiffness design method using a dynamic ARMA model, and (iii) to formulate a new probabilistic multi-objective optimal design problem.

In this paper, mechanically meaningful quantities, i.e., story stiffness, girder-to-column stiffness ratio and ratio of moment-resisting frame stiffness to the total story stiffness (frame participation ratio), are adopted as the principal parameters to directly determine the member size. It is therefore easy to reflect the designer's experience and intuition and to construct an interactive decision making environment between the designer and a computer. Several frames designed via this stiffness-oriented design method are then subjected to three kinds of design disturbances; to gravity loading alone, to combined gravity and moderate earthquake loading, and to combined gravity and severe earthquake loading. Then a general probabilistic multi-objective optimal design method is proposed. Step-by-step nonlinear time history analysis is used in the multi-objective optimal design method to simulate a complete probabilistic distribution of inelastic peak responses. In spite of the development of nonlinear random vibration theory, it seems too difficult to estimate the complete probabilistic distribution of inelastic peak responses, which is necessary to quantify the exact reliability of a structure, without carrying out the inelastic time history analysis [4–6]. Although the practicality of this approach may be argued by structural engineers, practicality is an increasingly relative concept, given dramatic improvements in computing.

A survey of optimal design methods for building structures under seismic loading can be found in [1, 7]. Literature relating directly to the present research will be referenced in the sequel.

As for the stiffness design method, Nakamura and Takenaka [8] developed an optimal design method for overall elastic compliance under static loading and proposed a closed form optimal design formula. Nakamura and Takewaki [9] introduced a new system performance parameter, called system flexibility, for a nonlinear building frame and formulated a ductility design method under a simplified dynamic loading condition. The elastic-response specified design method for space trusses has been formulated by Nakamura and Ohsaki [10] also under a simplified dynamic loading condition.

Several *elastic* design methods have been proposed for optimal design of building structures using a fuzzy concept [11–15]. Almost all of these problems have been solved by utilizing conventional numerical optimization algorithms except [14].

At the University of California, Berkeley, much attention has been given to the use of optimization concepts for the development of rational seismic-resistant design methods. Multi-objective optimal design methods under seismic loading have been developed by Pister and his co-workers [16–24]. It is of great importance from the standpoint of reliability that they evaluate inelastic response by using time history analysis within the design process itself. Past works are summarized in [19, 23, 24].

2. DESIGN EARTHQUAKES

2.1. *Dynamic ARMA model*

Since the reliability of prediction of the probabilistic distribution of seismic structural response depends on modeling of the earthquake input motion, it is apparent that the development of a sophisticated model of design earthquakes is essential to the construction of a reliable earthquake-resistant design theory for building structures. A proper model of design earthquakes requires appropriate modeling and handling of several important factors, such as local site amplification factors, amplitude of motion, duration of strong shaking, frequency content, etc.

Although it is often the case that uncertainty associated with one of the factors described above correlates with that of another factor, uncertainty of the global ground motion parameters should be handled independently of uncertainty attached to the ground motion time history itself. The first type of uncertainty has to be handled using probabilistic seismic hazard analysis techniques. On the other hand, to model the second type of uncertainty, it is rational to regard ground motion as an outcome from an underlying stochastic process.

Dual criteria are used in this paper to take into account the first type of uncertainty based upon the *accepted design philosophy* [25, 26]. Design earthquakes with two different levels are then defined as the moderate earthquake and the severe earthquake, respectively. To model the second type of uncertainty, a dynamic ARMA model is employed here. The dynamic ARMA model acts as a simulator for generating a set of artificial earthquake ground motions statistically similar to the original recorded earthquake ground motion. The interested reader is referred to [27–30] for details of this dynamic ARMA model.

There have been several efforts to simulate earthquake ground motions by using ARMA models [27–29, 31–34]. These research works have clarified that ARMA models have the potential to successfully simulate recorded earthquake ground motions.

One of the principal advantages of using the dynamic ARMA model may be stated as follows. Since each ground motion sample generated by means of this dynamic ARMA model belongs to the same underlying stochastic process, no ground motion scaling needs to be done and the variability of the corresponding ground motion and structural response parameters is an inherent type of variability attached to the stochastic process of the design earthquake under consideration. In other words, this dynamic ARMA model makes it possible to gain insight into the inherent variability of the seismic structural response as propagated from the inherent source of uncertainty attached to the ground motion

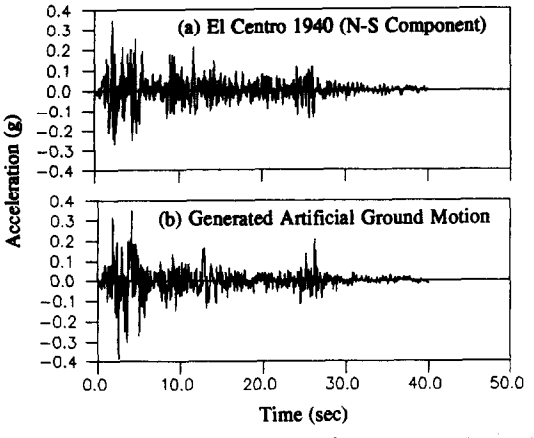

Fig. 1. (a) Recorded accelerogram of El Centro 1940 (N–S component). (b) Accelerogram of a generated artificial ground motion.

time history. Another advantage is that the use of this dynamic ARMA model facilitates the handling of temporal change of frequency content of a ground motion, which has been reported to be one of the most critical factors to influence the damage indices of a building (for example, see [29, 35]). The dynamic ARMA model also makes it possible to proceed directly and systematically from the analysis of historical discretized earthquake ground motion records to the synthesis of artificial discretized accelerograms with similar statistical properties. Furthermore, Chang *et al.* [32] have shown that there is a one-to-one correspondence between the continuous time model and the discrete time model. They actually presented a comparison table including transfer functions, autocorrelation functions and stability conditions. It is therefore easy to reflect the meaning of physical parameters in setting ARMA parameters.

Figure 1(a) shows the recorded accelerogram of El Centro 1940 (N–S component). On the other hand, the accelerogram of an artificial ground motion generated by means of the dynamic ARMA model [27, 29, 30] is plotted in Fig. 1(b). Kalman filtering has been utilized in estimating the ARMA parameters.

Figures 2(a) and (b) graph the mean value and the mean $\pm$ one standard deviation of acceleration response spectra and displacement response spectra, respectively, corresponding to a damping ratio of 3% for 100 generated artificial ground motions. The acceleration response spectrum with the level of mean plus one standard deviation will be used in the dynamic design method described in Sec. 4.

2.2. *Moderate earthquakes*

The peak ground acceleration of the original recorded earthquake ground motion is $0.348g$, where g is the acceleration of gravity, and the mean value of the peak ground accelerations of 100 generated artificial earthquakes is $0.353g$. In order to construct a set of design moderate earthquakes, the entire set of generated ground motions was uniformly scaled so that the mean value of the peak ground accelerations was $0.15g$.

2.3. *Severe earthquakes*

On the other hand, for the purpose of constructing a set of design severe earthquakes, the entire set of generated ground motions was uniformly scaled so that the mean value of the peak ground accelerations was $0.5g$.

3. DECOMPOSED STIFFNESS DESIGN METHOD

In designing a braced steel frame, one of the primary concerns is how to assign the ratio of the moment-resisting frame stiffness to the total story stiffness. In this section a new design method for concentrically braced steel frames is developed, which allows a designer to assign the ratio based upon his or her experience or in accordance with code recommendations.

3.1. *Design variables and element parameters*

In this paper, moment of inertia is the primary section property used for the girder and column elements in the simplified design method described below. Other element section properties, i.e., radius of gyration and cross-sectional depth, are obtained from empirical relations derived by Walker [36].

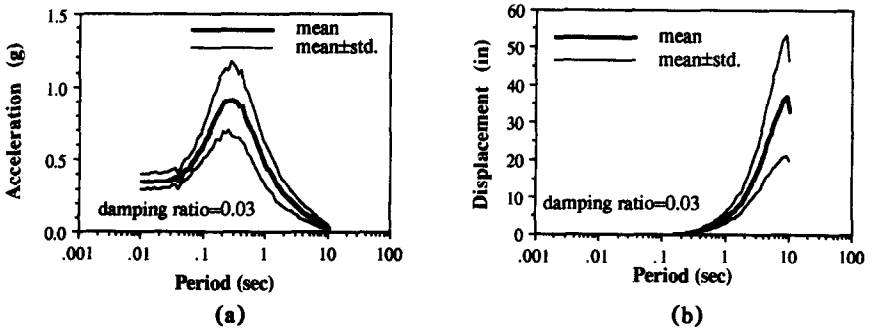

Fig. 2. Response spectra for 100 artificial earthquakes (mean value and mean $\pm$ one standard deviation). (a) Acceleration response spectrum (damping ratio = 3%). (b) Displacement response spectrum (damping ratio = 3%).

These relations have been derived from a least-square fit of data corresponding to the 'economy' wide-flange sections among the American Institute of Steel Construction standard hot rolled shapes. The relationships are expressed as follows (in Imperial units):

for columns with $I \leqslant 429$ in.^{4}

$$d = 1.47I^{0.368},$$
$$r = 0.39d^{1.04} \tag{1}$$

for columns with $I \geqslant 429$ in.^{4}

$$d = 10.5I^{0.0436},$$
$$r = 0.39d^{1.04} \tag{2}$$

for girders,

$$d = 2.66I^{0.287},$$
$$r = 0.52d^{0.920}, \tag{3}$$

where I is the moment of inertia (section second moment of area) (in.^{4}), d, the section depth (in.), and r, the section radius of gyration (in.).

The cross-sectional area and fully plastic moment can then be computed as follows:

$$A = I/r^2 \tag{4}$$

$$M_p = \sigma_y(Ad/8 + 3I/2d), \tag{5}$$

where A is the cross-sectional area, M_p is the fully plastic moment, and σ_y is the yield stress.

On the other hand, cross-sectional area is the primary section property for the bracing elements and the moment of inertia of a bracing member can be expressed in terms of the cross-sectional area as follows:

$$I = 0.169A^3. \tag{6}$$

3.2. *Design problem*

In Sec. 3, the following design problem is considered: Given the geometrical parameters concerned with location of frame nodes and the mechanical properties of constituent materials, find the moments of inertia of columns and girders and the cross-sectional areas of bracing members of the frame which shows the specified response to a set of static lateral loads and where the ratio of moment-resisting frame stiffness to the total story stiffness is specified.

The types of response specification will be classified in three groups in the following sections.

3.3. *One-bay model (original case)*

Consider an f-story one-bay braced frame, shown in Fig. 3, which is subjected to a set of horizontal design loads $\{H_j\}$ as computed in accordance with the UBC code [37]. Let L, h_j, and E denote the span length, the height of jth story and Young's modulus of materials consisting of girders, columns and braces, respectively. These parameters are to be prescribed throughout the design process. Let θ_j, R_j denote the angle of rotation of the joint node in the jth floor and the angle of member rotation of the column in the jth story, respectively. It should be noted that these angles represent the deformation under horizontal loads alone. In Secs 3 and 4 columns are assumed to be inextensional. This assumption gives a first-order approximation of the behavior of a concentrically braced frame and leads to a relatively good estimate of the behavior of a low-rise building frame to lateral loading. Since the design formula derived in this section is used only as a tool for determining member size in Sec. 5, this assumption does not create any problem in the multi-objective optimal design method described in Sec. 5.

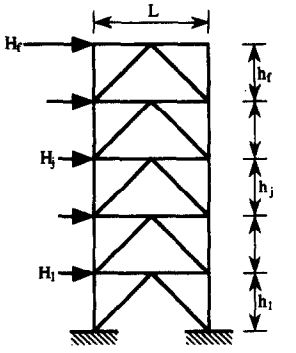

Fig. 3. Multi-story one-bay braced steel frame.

In this section the following design problem is considered: Given L, h_j, and E, find the moments of inertia of girders $\{I_{Bj}\}$, those of columns $\{I_{Cj}\}$ and the cross-sectional areas of braces $\{A_{bj}\}$ of the frame which shows the specified response, $\theta_j = \bar{\theta}$ and $R_j = q_j\bar{R}$, to the design lateral loads $\{H_j\}$ and where the story shear forces sustained by the moment-resisting frame are specified by $\zeta_j Q_j = p_j\bar{\zeta}Q_j$. The coefficients q_j and p_j are the prescribed parameters. It should be noted that this idea is based upon the concept of 'response constrained design' due to Nakamura and his co-workers (for example, see [38, 39]).

The total story shear force Q_j in the jth story can be expressed as the sum of the shear force Q_{Fj} sustained by the moment-resisting frame and that Q_{Xj} by the bracing system

$$Q_j = Q_{Fj} + Q_{Xj}. \tag{7}$$

Q_{Fj} and Q_{Xj} are expressed as follows in terms of the member forces

$$Q_{Fj} = \frac{2}{h_j}(M_{Cj}^U + M_{Cj}^L) \tag{8}$$

$$Q_{Xj} = 2N_j \cos\gamma_j, \tag{9}$$

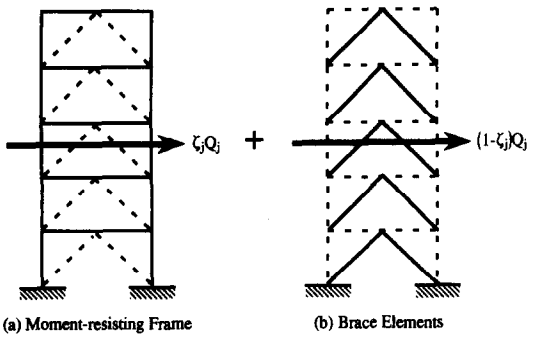

Fig. 4. Story shear participation.

where M_{Cj}^U, M_{Cj}^L, N_j denote the bending moments at upper and lower ends of the jth column and the axial force of the bracing member in the jth story, respectively, and γ_j denotes the angle between the bracing member and the floor girder in the jth story.

In this paper a new design method called 'decomposed stiffness design method' is developed. The characteristic feature of this method is to treat the moment-resisting frame and the bracing system independently. The procedure for deriving the moments of inertia of columns and girders and the cross-sectional areas of bracing members will be presented next.

Moment-resisting frame. Since the story shear force Q_{Fj} sustained by the moment-resisting frame is prescribed as $\zeta_j Q_j$ (see Fig. 4a), eqn (8) can be reduced to

$$\frac{2}{h_j}(M_{Cj}^U + M_{Cj}^L) = \zeta_j Q_j. \tag{10}$$

The moment equilibrium equation at the joint node in the jth floor provides

$$M_{Bj} = M_{Cj}^U + M_{Cj+1}^L, \tag{11}$$

where M_{Bj} denotes the bending moment at the member end of the girder in the jth floor. On the other hand, the member stiffness matrices provide the following relations

$$M_{Cj}^L = \frac{2EI_{Cj}}{h_j}(3R_j - 2\theta_{j-1} - \theta_j) \tag{12}$$

$$M_{Cj}^U = \frac{2EI_{Cj}}{h_j}(3R_j - 2\theta_j - \theta_{j-1}) \tag{13}$$

$$M_{Bj} = \frac{6EI_{Bj}}{L}\theta_j. \tag{14}$$

Substitution of eqns (12) and (13) into (10) yields

$$\frac{12EI_{Cj}}{h_j^2}(2R_j - \theta_{j-1} - \theta_j) = \zeta_j Q_j. \tag{15}$$

Furthermore, substitution of eqns (12)–(14) into (11) provides the following equation

$$\frac{6EI_{Bj}}{L}\theta_j = \frac{2EI_{Cj}}{h_j}(3R_j - 2\theta_j - \theta_{j-1}) + \frac{2EI_{Cj+1}}{h_{j+1}}(3R_{j+1} - 2\theta_j - \theta_{j+1}). \tag{16}$$

In this paper the following response specification is initially adopted to simplify the design procedure

$$R_j = q_j \bar{R} \tag{17}$$

$$\theta_j = \text{const.} = \bar{\theta} \tag{18}$$

$$\zeta_j = p_j \bar{\zeta}. \tag{19}$$

If the ratio of $\bar{\theta}$ to $\bar{R}$ is denoted by r, substitution of eqns (17)–(19) into (15) and (16) furnishes the following expressions

$$\frac{24EI_{Cj}}{h_j^2}(q_j - r)\bar{R} = p_j \bar{\zeta} Q_j, \quad (j \neq 1) \tag{20}$$

$$\frac{6EI_{Bj}}{L} r\bar{R} = \frac{\bar{\zeta}}{4}(p_j Q_j h_j + p_{j+1} Q_{j+1} h_{j+1}), \quad (j \neq 1). \tag{21}$$

The moments of inertia of columns and girders may then be obtained from eqns (20) and (21) as follows:

$$I_{Cj} = \frac{p_j \bar{\zeta} Q_j h_j^2}{24E(q_j - r)\bar{R}}, \quad (j \neq 1) \tag{22}$$

$$I_{C1} = \frac{p_1 \bar{\zeta} Q_1 h_1^2}{24E(q_1 - 0.5r)\bar{R}} \tag{23}$$

$$I_{Bj} = \frac{L\bar{\zeta}}{24Er\bar{R}}(p_j Q_j h_j + p_{j+1} Q_{j+1} h_{j+1}), \quad (j \neq 1) \tag{24}$$

$$I_{B1} = \frac{L\bar{\zeta}}{24Er\bar{R}}\left\{\frac{(3q_1 - 2r)}{(3q_1 - 1.5r)} p_1 Q_1 h_1 + p_2 Q_2 h_2\right\}. \tag{25}$$

It should be noted that I_{C1} and I_{B1} have been derived independently of eqns (20) and (21). This is due to the boundary effect.

In this case, the ratio of I_{Bj} to I_{Cj} may be expressed as follows:

$$\frac{I_{Bj}}{I_{Cj}} = \frac{q_j - r}{r}\frac{(p_j Q_j h_j + p_{j+1} Q_{j+1} h_{j+1})}{p_j Q_j h_j}\frac{L}{h_j}, \quad (j \neq 1). \tag{26}$$

Equation (26) indicates that the ratio I_{Bj}/I_{Cj} approaches ∞ as r approaches 0 and the ratio I_{Bj}/I_{Cj} approaches 0 as r approaches q_j. This characteristic provides useful information for specification of $\bar{\theta}$ and $\bar{R}$.

Bracing system. Since the story shear force Q_{Xj} sustained by the bracing system is prescribed as $(1-\zeta_j)Q_j$ (see Fig. 4b), eqn (9) can be rewritten as

$$2N_j \cos\gamma_j = (1-\zeta_j)Q_j. \tag{27}$$

The member stiffness relation of the bracing system yields

$$N_j = \frac{2EA_{bj}h_j\cos^2\gamma_j}{L}R_j. \tag{28}$$

Substitution of eqn (28) into (27) provides the following equation

$$\frac{4EA_{bj}h_jR_j\cos^3\gamma_j}{L} = (1-\zeta_j)Q_j. \tag{29}$$

The cross-sectional area A_{bj} of the bracing member can be obtained by substituting eqns (17) and (19) into (29)

$$A_{bj} = \frac{L(1-p_j\bar{\zeta})Q_j}{4Eh_jq_j\bar{R}\cos^3\gamma_j}. \tag{30}$$

In typical structural design practice, it may be preferable to assign the same stiffness to a group of members. This requirement results from convenience in construction and/or economics. As a simple example, a four-story one-bay braced frame is considered here and two cases are dealt with. It should be noted that although only the essence of the formulation is shown here, the extension of the present formulation to frames with a different number of stories is straightforward.

3.4. *One-bay model (design variable grouping [case 1])*

The columns and bracing members in each two stories have the same stiffness as shown in Fig. 5(b). The design variables are now $I_{C1}, I_{C3}, I_{B1}, \ldots, I_{B4}$, A_{b1}, A_{b3}. In this case it is assumed that the stories with the same moment of inertia of columns (and the same cross-sectional area of bracing members) have a common story height; $h_2 = h_1$ and $h_4 = h_3$ in this example. Since the number of design variables has decreased, it is only possible to specify a smaller number of response parameters. The following response specification is employed here as an example

$$\theta_j = \bar{\theta}, \tag{31}$$

$$(R_1 + R_2)/2 = q_1\bar{R}, \tag{32}$$

$$(R_3 + R_4)/2 = q_3\bar{R}, \tag{33}$$

$$\zeta_1Q_1 + \zeta_2Q_2 = p_1\bar{\zeta}(Q_1+Q_2), \tag{34}$$

$$\zeta_3Q_3 + \zeta_4Q_4 = p_3\bar{\zeta}(Q_3+Q_4), \tag{35}$$

where q_1, q_3, p_1, p_3 are the prescribed parameters. Equations (34) and (35) mean that the moment-resisting frame participation ratio in story shear forces is specified, with the story shear forces acting as weighting coefficients.

Moment-resisting frame. Equations corresponding to eqns (15) can be written as follows after substituting (31)

$$\frac{12EI_{C1}}{h_1^2}(2R_1 - \bar{\theta}) = \zeta_1Q_1 \tag{36}$$

$$\frac{12EI_{C1}}{h_1^2}(2R_2 - 2\bar{\theta}) = \zeta_2Q_2 \tag{37}$$

$$\frac{12EI_{C3}}{h_3^2}(2R_3 - 2\bar{\theta}) = \zeta_3Q_3 \tag{38}$$

$$\frac{12EI_{C3}}{h_3^2}(2R_4 - 2\bar{\theta}) = \zeta_4Q_4. \tag{39}$$

The moment of inertia of columns I_{C1} can be obtained by summing up eqns (36) and (37) and substituting eqns (32) and (34) for response specification into the resulting equation

$$I_{C1} = \frac{p_1\bar{\zeta}(Q_1+Q_2)h_1^2}{48E(q_1 - 0.75r)\bar{R}}. \tag{40}$$

In the same way, I_{C3} can be obtained as

$$I_{C3} = \frac{p_3\bar{\zeta}(Q_3+Q_4)h_3^2}{48E(q_3 - r)\bar{R}}. \tag{41}$$

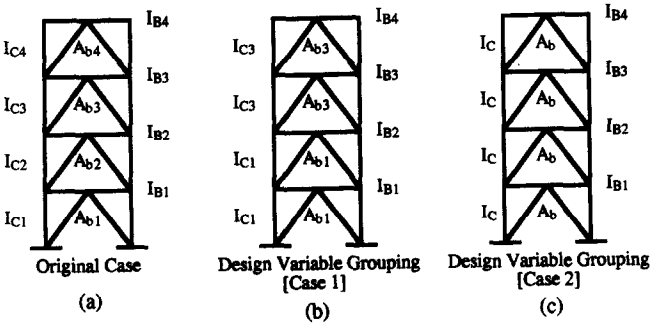

Fig. 5. Grouping of design variables.

The equation corresponding to eqn (24) is expressed as

$$I_{Bj} = \frac{L}{24Er\bar{R}}(\zeta_j Q_j h_j + \zeta_{j+1} Q_{j+1} h_{j+1}), \quad (j \neq 1). \tag{42}$$

I_{B1} can be obtained by considering the boundary effect

$$I_{B1} = \frac{Lh_1 p_1 \bar{\zeta}(Q_1 + Q_2)(6q_1 - 5r)}{144Er\bar{R}(q_1 - 0.75r)}. \tag{43}$$

The angles of member rotation of columns can be expressed in terms of ζ_1–ζ_4 from eqns (32) and (33) for response specification and eqns (36)–(39)

$$R_1 = \frac{(2q_1 - r)\zeta_1 Q_1 + 0.5r\zeta_2 Q_2}{p_1\bar{\zeta}(Q_1 + Q_2)}\bar{R} \tag{44}$$

$$R_2 = \frac{r\zeta_1 Q_1 + (2q_1 - 0.5r)\zeta_2 Q_2}{p_1\bar{\zeta}(Q_1 + Q_2)}\bar{R} \tag{45}$$

$$R_3 = \frac{(2q_3 - r)\zeta_3 Q_3 + r\zeta_4 Q_4}{p_3\bar{\zeta}(Q_3 + Q_4)}\bar{R} \tag{46}$$

$$R_4 = \frac{r\zeta_3 Q_3 + (2q_3 - r)\zeta_4 Q_4}{p_3\bar{\zeta}(Q_3 + Q_4)}\bar{R}. \tag{47}$$

Bracing system. The equations corresponding to eqns (29) can be expressed as follows:

$$A_{b1} R_1 = \frac{L(1 - \zeta_1)Q_1}{4Eh_1 \cos^3 \gamma_1} \tag{48}$$

$$A_{b1} R_2 = \frac{L(1 - \zeta_2)Q_2}{4Eh_1 \cos^3 \gamma_1} \tag{49}$$

$$A_{b3} R_3 = \frac{L(1 - \zeta_3)Q_3}{4Eh_3 \cos^3 \gamma_3} \tag{50}$$

$$A_{b3} R_4 = \frac{L(1 - \zeta_4)Q_4}{4Eh_3 \cos^3 \gamma_3}. \tag{51}$$

The cross-sectional area A_{b1} of the first- and second-story bracing members can be obtained by summing up two eqns (48) and (49) and substituting eqns (32) and (34) for response specification into the resulting equation

$$A_{b1} = \frac{L(Q_1 + Q_2)(1 - p_1\bar{\zeta})}{8q_1\bar{R}Eh_1 \cos^3 \gamma_1}. \tag{52}$$

In the same way, the cross-sectional area A_{b3} of the third- and fourth-story bracing members can be obtained as

$$A_{b3} = \frac{L(Q_3 + Q_4)(1 - p_3\bar{\zeta})}{8q_3\bar{R}Eh_3 \cos^3 \gamma_3}. \tag{53}$$

The angles of member rotation of columns can be expressed in terms of ζ_1–ζ_4 by substituting eqns (40) and (41) into eqns (36)–(39)

$$R_1 = \frac{2q_1(1 - \zeta_1)\bar{R}Q_1}{(Q_1 + Q_2)(1 - p_1\bar{\zeta})} \tag{54}$$

$$R_2 = \frac{2q_1(1 - \zeta_2)\bar{R}Q_2}{(Q_1 + Q_2)(1 - p_1\bar{\zeta})} \tag{55}$$

$$R_3 = \frac{2q_3(1 - \zeta_3)\bar{R}Q_3}{(Q_3 + Q_4)(1 - p_3\bar{\zeta})} \tag{56}$$

$$R_4 = \frac{2q_3(1 - \zeta_4)\bar{R}Q_4}{(Q_3 + Q_4)(1 - p_3\bar{\zeta})} \tag{57}$$

A set of simultaneous equations for ζ_1–ζ_4 can be constructed by equating eqns (44)–(47) and (54)–(57). The solution to the equations can be expressed as follows:

$$\zeta_1 = \frac{\{4q_1 Q_1 - r(1 - p_1\bar{\zeta})(Q_1 + Q_2)\}p_1\bar{\zeta}}{\{4q_1 - 3r(1 - p_1\bar{\zeta})\}Q_1} \tag{58}$$

$$\zeta_2 = \frac{\{4q_1 Q_2 - 2r(1 - p_1\bar{\zeta})(Q_1 + Q_2)\}p_1\bar{\zeta}}{\{4q_1 - 3r(1 - p_1\bar{\zeta})\}Q_2} \tag{59}$$

$$\zeta_3 = \frac{\{2q_3 Q_3 - r(1 - p_3\bar{\zeta})(Q_3 + Q_4)\}p_3\bar{\zeta}}{2\{q_3 - r(1 - p_3\bar{\zeta})\}Q_3} \tag{60}$$

$$\zeta_4 = \frac{\{2q_3 Q_4 - r(1 - p_3\bar{\zeta})(Q_3 + Q_4)\}p_3\bar{\zeta}}{2\{q_3 - r(1 - p_3\bar{\zeta})\}Q_4}. \tag{61}$$

These expressions of ζ_1–ζ_4 have to be substituted into eqn (42) to obtain the final form of I_{Bj}.

3.5. *One-bay model (design variable grouping [case 2])*

Consider an alternative case where all the columns have the same moment of inertia and all the bracing members have the same cross-sectional area (see Fig. 5c). To derive analytical expressions, it is assumed that all the stories have a common story height. The design variables are now $I_C, I_{B1}, \ldots, I_{B4}, A_b$. In this case the following response specification is possible

$$\theta_j = \bar{\theta}, \tag{62}$$

$$(R_1 + R_2 + R_3 + R_4)/4 = \bar{R}, \tag{63}$$

$$\zeta_1 Q_1 + \zeta_2 Q_2 + \zeta_3 Q_3 + \zeta_4 Q_4 = \bar{\zeta}(Q_1 + Q_2 + Q_3 + Q_4). \tag{64}$$

The moment of inertia of columns I_C can be obtained by summing up the equations corresponding to eqns (36)–(39) and applying the conditions, eqns (63) and (64). The moments of inertia of girders, I_{Bj} $(j \neq 1)$ and I_{B1}, can be derived in almost the same

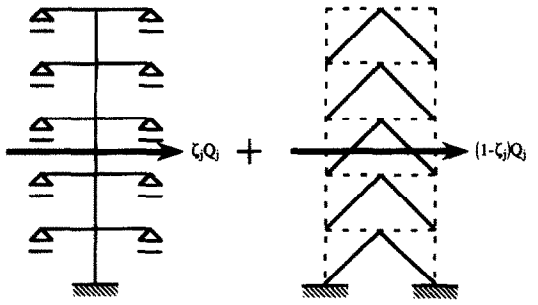

Fig. 6. Subassemblage model representation of a moment-resisting frame.

manner as in [23]. Furthermore R_1–R_4 and ζ_1–ζ_4 can be obtained from the horizontal equilibrium equations corresponding to eqns (36)–(39), the expression for I_C and eqn (63).

3.6. *Multi-bay model*

Consider an f-story subassemblage model, shown in Fig. 6, which may be regarded as a part of a multi-bay frame. Let L, h_j, and E denote the prescribed distance between the two roller supports at the same floor level, the prescribed story height of the jth story and Young's modulus of constituent materials, respectively.

The governing equilibrium equations are the same as those for a one-bay frame model except that the member-end bending moments in columns are doubled. Therefore the stiffness of each column has to be twice that of a one-bay frame model. It should be noted here that the story shear forces divided by the number of bays have to be employed as those applied to the subassemblage model.

To extend the design formula for a subassemblage model to that for a multi-bay model, it is straightforward to adopt the following transformation procedure. The interior columns of the multi-bay frame are to have the same stiffness as those of the subassemblage model. On the other hand, the exterior columns of the former frame are to have half the stiffness of the columns of the latter frame. As for girders, it is reasonable to assign the stiffnesses so that the girders of the former frame have the same equivalent stiffnesses as those of the latter frame where 'equivalent stiffness' means moment of inertia of a member divided by its length.

4. DECOMPOSED STIFFNESS DESIGN METHOD FOR DYNAMIC LOADING

In Sec. 3, a design formula was proposed for equivalent static lateral loads. To make this design formula more effective under dynamic loading, the design lateral loads need to be evaluated based on the dynamic characteristics of the design earthquakes and the structure. The SRSS (Square Root of Sum of the Squares) procedure provides an estimate for evaluating the mean peak responses of an elastic structure to a set of earthquake ground motions. In this paper, an iterative procedure is employed to find the design which exhibits the specified mean peak responses to the design moderate earthquakes. The flow diagram for this dynamic design method is shown in Fig. 7. As indicated in Fig. 7, the design lateral loads in the UBC code are adopted only in the first iteration cycle. This is because the member stiffnesses of a frame have to be specified in utilizing the SRSS procedure and the story shear forces evaluated by the SRSS method are available from the second design cycle.

The mean peak story shear forces are calculated using the SRSS procedure as follows:

$$Q_j = \left[\sum_{r=1}^{n_T} \left\{ v^{(r)} S_A(T_r; h_r) \sum_{i=j}^{f} m_i \phi_i^{(r)} \right\}^2 \right]^{1/2}, \quad (65)$$

where $v^{(r)}$ is the participation factor of the rth mode; T_r, rth natural period; $S_A(T; h)$, acceleration response spectrum; h_r, rth damping ratio; m_i, mass at ith floor level; $\phi_i^{(r)}$, ith component of rth eigenvector; and n_T, number of adopted modes. In eqn (65), the acceleration response spectrum $S_A(T; h)$ is to be constructed from a set of earthquakes generated by the dynamic ARMA model.

This design method incorporating the dynamic evaluation procedure of design forces into the stiffness-oriented static design formula will be called the 'dynamic stiffness design method' and the frame designed by this dynamic stiffness design method will be called the 'dynamic stiffness design' in the sequel. It is important to note that once a parameter set $(\bar{R}, r, \zeta)$ is specified, the moments of inertia of columns and girders and the cross-sectional areas of bracing members are determined.

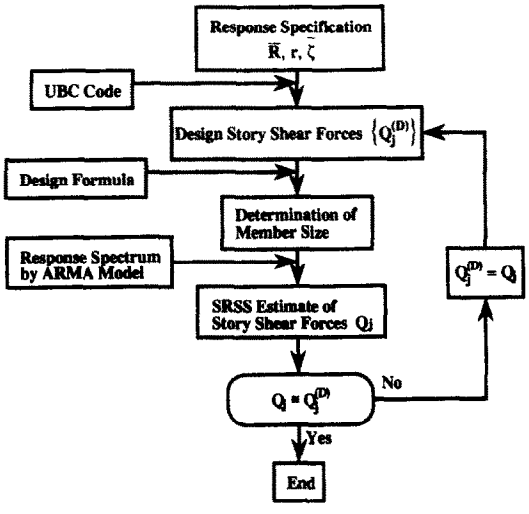

Fig. 7. Flow diagram for dynamic stiffness design method using ARMA model.

It should be noted further that the validity of the SRSS technique is justified only when applied for an earthquake input motion process that is stationary and Gaussian [40]. Since the set of moderate earthquakes generated here has nonstationary characteristics, the mean peak response of the frame designed based on this method may not satisfy the requirement. However, the procedure used here only provides an initial approximation for determining the member size of the frame, which is to be designed by a more general design procedure based upon the sensitivity concept in the multi-objective optimal design problem presented in the next section. It should be noted that there is no reliable technique available to estimate the mean peak response of an elastic structure to a set of design earthquakes with nonstationary characteristics, except by carrying out time history analysis.

5. PROBABILISTIC MULTI-OBJECTIVE OPTIMAL DESIGN METHOD

At present, there is a general consensus in structural design practice that an earthquake-resistant structure should:

(a) resist minor earthquakes without damage;
(b) resist moderate earthquakes without structural damage, but possibly with limited non-structural damage;
(c) resist severe earthquakes without collapse, but possibly with limited structural damage.

This criterion is often referred to as the 'accepted design philosophy' [25, 26]. In this section a new probabilistic multi-objective optimal design method is developed based upon this criterion.

5.1. *Constraints under gravity loads alone (limit state 1)*

Constraints on the response of the frame under gravity loads alone (see Fig. 8a) are imposed to insure structural integrity and functionality. The constraints may be expressed as follows:

$$|\text{column axial force}| < \text{Colax} \times \text{Column axial yield force} \quad (66)$$

$$|\text{column end moment}| < \text{Colgra} \times \text{Column yield moment} \quad (67)$$

$$|\text{girder end moment}| < \text{Girgra} \times \text{Girder yield moment} \quad (68)$$

$$|\text{girder midspan deflection under gravity load}| < \text{Girdef} \times \text{Girder span}. \quad (69)$$

Colax, Colgra, Girgra, and Girdef in eqns (66)–(69) represent the [Good, Bad] pair for each response. The detailed description of such parameters will be given in Sec. 5.6.

5.2. *Constraints under combined gravity and moderate earthquake loads (limit state 2)*

The accepted design philosophy suggests that structural damage should be avoided under moderate earthquake loading (see Fig. 8b). This requirement may be satisfied by imposing the following constraints

$$|\text{column end moment}|_{\max \text{ over time}} < \text{Colyld} \times \text{Column yield moment} \quad (70)$$

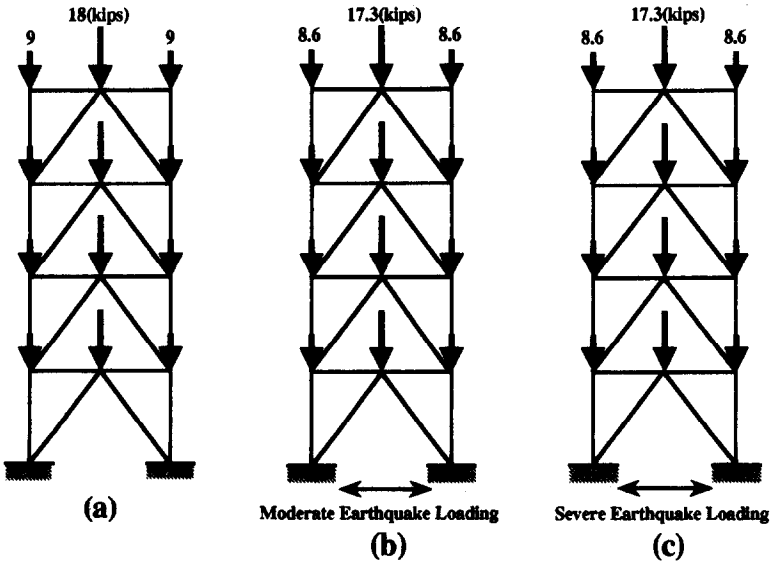

Fig. 8. Three limit states. (a) Limit state 1 (under gravity loads alone). (b) Limit state 2 (under combined gravity and moderate earthquake loading). (c) Limit state 3 (under combined gravity and severe earthquake loading).

$$|\text{girder end moment}|_{\max \text{ over time}} < \text{Giryld} \times \text{Girder yield moment} \quad (71)$$

$$|\text{brace axial force}|_{\max \text{ over time}} < \text{Brayld} \times \text{Brace yield axial force.} \quad (72)$$

Non-structural damage, such as cracking of glass and plaster, will be controlled by setting the following constraint

$$|\text{story drift}|_{\max \text{ over time}} < \text{Drift} \times \text{Story height.} \quad (73)$$

Furthermore, the damage of equipment attached to floors will be controlled by the following requirement

$$|\text{absolute floor acceleration}|_{\max \text{ over time}} < \text{Accel} \times \text{Acceleration of gravity.} \quad (74)$$

Colyld, Giryld, Brayld, Drift, and Accel represent the [Good, Bad] pair for each response. The explanation of such parameters will be given in Sec. 5.6.

5.3. *Constraints under combined gravity and severe earthquake loads (limit state 3)*

According to the accepted design philosophy, structural collapse should be avoided under severe earthquake loading (see Fig. 8c). The following constraint is chosen to control the overall behavior of the frame

$$|\text{frame sway}|_{\max \text{ over time}} < \text{Sway} \times \text{Frame height.} \quad (75)$$

On the other hand, some structural damage is allowable during severe earthquake loading. The extent of the damage will be controlled by limiting the member deformation. For this purpose, the following constraints are imposed to keep the structural damage within an allowable range

$$\text{column end accumulated plastic hinge rotation ductility} < \text{Colduc} \quad (76)$$

$$\text{girder end accumulated plastic hinge rotation ductility} < \text{Girduc} \quad (77)$$

$$\text{brace accumulated plastic extension ductility} < \text{Braduc.} \quad (78)$$

Sway, Colduc, Girduc, and Braduc represent the [Good, Bad] pairs for this limit state. These parameters will also be explained in Sec. 5.6.

5.4. *Box constraints*

Box constraints are introduced so that the girder and column moments of inertia are constrained to lie within the intervals [80 in.^{4}, 2500 in.^{4}] and [50 in.^{4}, 4500 in.^{4}]. Brace element cross-sectional areas are constrained to lie within the interval [0.5 in.^{2}, 10 in.^{2}]. If some of the moments of inertia and cross-sectional areas obtained using the dynamic stiffness design method are out of the intervals, the corresponding lower or upper bounds described before are adopted in the multi-objective optimal design method.

5.5. *Response simulation model and method*

The general purpose structural analysis program DRAIN-2D [41] is used to compute the structural response for each limit state.

The beam and column elements are bare wide flange sections and are modeled using lumped-plasticity parallel-component elements in DRAIN-2D. These sections are assumed to be compact and sufficiently restrained so that lateral and local buckling failures are delayed until after the development of required plastic hinge rotations. Shearing deformation and out-of-plane deformations were not considered in order to simplify the analysis. Likewise, the finite size of the beam–column joints was disregarded, as were panel zone deformations. Moreover, the yield stress σ_y was set to 36 ksi, Young's modulus E to 29,000 ksi and the strain-hardening ratio to 0.05. For the columns, geometric nonlinearities were taken into account and an AISC-based axial force versus bending moment interaction yield condition [42] was used. The balancing points are $(M/M_Y, N/N_Y) = (1.0, 0.15), (-1.0, 0.15), (1.0, -0.15), (-1.0, -0.15)$.

The bracing members are modeled using truss elements in DRAIN-2D (see Fig. 9). This element exhibits hysteretic behavior in tension only. In compression the element is assumed to buckle at the critical stress which is computed according to the following formula [3]

$$\sigma_{CR} = \frac{\pi^2 E}{(kL/r)^2} \quad \text{for} \quad C_c < \frac{kL}{r} \quad (79a)$$

$$\sigma_{CR} = \sigma_y \left[1 - \frac{(kL/r)^2}{2C_c^2} \right] \quad \text{for} \quad \frac{kL}{r} \leqslant C_c \quad (79b)$$

in which

$$C_c = \sqrt{\left(\frac{2\pi^2 E}{\sigma_y} \right)}. \quad (80)$$

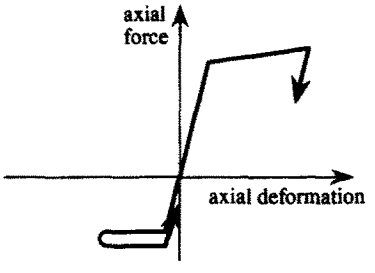

Fig. 9. Axial force–axial deformation relationship of a bracing member (DRAIN-2D).

Geometric nonlinearities were taken into account. The yield stress σ_y was set to 36 ksi, Young's modulus E to 29,000 ksi and the strain-hardening ratio to 0.005.

The Rayleigh damping model with 3% damping in the first and second modes was assumed with additional damping during large amplitude motions taken into account by including the material's hysteretic behavior in nonlinear time history analysis. The damping matrix adopted here is expressed as follows:

$$[C] = \alpha[M] + \beta[K] \tag{81}$$

where $[C]$, $[M]$, and $[K]$ are a damping matrix, a mass matrix, and an initial stiffness matrix, respectively, and α, β represent the following values

$$\alpha = \frac{2\lambda\omega_1\omega_2}{\omega_1 + \omega_2} \tag{82a}$$

$$\beta = \frac{2\lambda}{\omega_1 + \omega_2} \tag{82b}$$

ω_1, ω_2 are the first and second natural circular frequencies and λ is the damping ratio in the first and second modes.

Finally, a Newmark's step-by-step integration scheme was used with the parameters set to give constant acceleration with no numerical damping. Each time history analysis had 4000 time steps of 0.01 sec.

5.6. *Description of dissatisfaction level for constraints*

Almost all of the constraints imposed within usual structural design practice have the following characteristics: The bounding value specifying the response performance is 'soft', and not always clear. It therefore seems reasonable to define an interval for each constraint [43, 44]. In this paper [Good, Bad] pairs are used to represent a designer's dissatisfaction level following Nye [43], Nye and Tits [44] and Austin *et al.* [19–21]. Recently this approach has been discussed for engineering design environments (for example, see [45]). If the response value corresponding to the specified exceedance probability is denoted by Resp, then the corresponding dissatisfaction level D is defined as follows:

$$D = 0, \quad \text{if Resp} < \text{Good} \tag{83a}$$

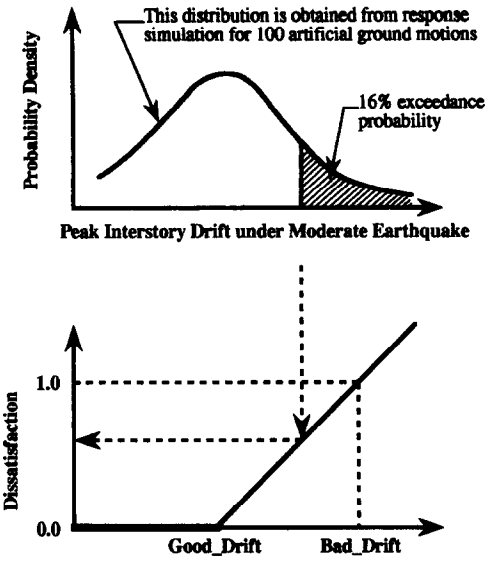

Fig. 10. Relationship of the probabilistic distribution of peak responses to the [Good, Bad] response values and evaluation of performance dissatisfaction level.

$$D = \frac{\text{Resp} - \text{Good}}{\text{Bad} - \text{Good}} \quad \text{otherwise,} \tag{83b}$$

where Good and Bad are the good and bad values of the response under consideration. The relationship of the probabilistic distribution of peak responses to the [Good, Bad] response values and the procedure for evaluation of performance dissatisfaction level are illustrated in Fig. 10. The [Good, Bad] pair for each constraint is shown in Table 1. A detailed explanation of these [Good, Bad] response values is given in [19].

5.7. *Definition of accumulated plastic deformation ductility ratio*

Although the total volume of a frame is often used as a convenient index measuring the initial cost of the frame, it seems quite difficult to define a [Good, Bad] pair for the total volume. This is because a structural engineer usually employs this parameter as a relative index and picks up a better design among several design candidates according to this index. In addition, it is questionable whether the total volume or total cost could be used as an appropriate index in a structure consisting of members with different load-carrying systems, such as braced frames. For this reason, another indicator is introduced in this paper

Table 1(a). Gravity loads alone constraint parameters

Parameter	Value	Description
Good_Colax	0.5	Good gravity column axial force factor
Bad_Colax	0.6	Bad gravity column axial force factor
Good_Colgra	0.6	Good gravity column yield factor
Bad_Colgra	0.8	Bad gravity column yield factor
Good_Girgra	0.6	Good gravity girder yield factor
Bad_Girgra	0.8	Bad gravity girder yield factor
Good_Girdef	1/240	Good girder midspan deflection
Bad_Girdef	1/219	Bad girder midspan deflection

Table 1(b). Combined gravity and moderate earthquake loading constraint parameters

Parameter	Value	Description
Good_Drift	0.005	Good maximum moderate story drift
Bad_Drift	0.008	Bad maximum moderate story drift
Good_Accel	0.7	Good maximum moderate floor acceleration in gs
Bad_Accel	1.4	Bad maximum moderate floor acceleration in gs
Good_Colyld	0.85	Good moderate column yield factor
Bad_Colyld	1.10	Bad moderate column yield factor
Good_Giryld	0.90	Good moderate girder yield factor
Bad_Giryld	1.10	Bad moderate girder yield factor
Good_Brayld	0.90	Good moderate brace yield factor
Bad_Brayld	1.10	Bad moderate brace yield factor

Table 1(c). Combined gravity and severe earthquake loading constraint parameters

Parameter	Value	Description
Good_Sway	0.014	Good overall sway
Bad_Sway	0.020	Bad overall sway
Good_Colduc	3.0	Good column accumulated p.h.r. ductility
Bad_Colduc	4.0	Bad column accumulated p.h.r. ductility
Good_Girduc	4.0	Good girder accumulated p.h.r. ductility
Bad_Girduc	6.0	Bad girder accumulated p.h.r. ductility
Good_Braduc	2.0	Good brace accumulated plastic extension ductility
Bad_Braduc	4.0	Bad brace accumulated plastic extension ductility

(p.h.r.: plastic hinge rotation)

to encourage the structural engineer to look for a design with smaller total volume. This concept is based on the accepted design philosophy according to which, from the standpoint of cost, limited inelastic response is allowed and desired under severe earthquakes. In this paper the following accumulated plastic deformation ductility ratio P_r is newly defined and used as an index to measure the ratio of the total amount of accumulated plastic deformation in a frame under severe earthquake loading to the sum of member capacities

$$P_r = \frac{\left[\sum_{i=1}^{n_c} \frac{\theta_{Pci}}{\theta_{Yci}} + \sum_{i=1}^{n_b} \frac{\theta_{Pbi}}{\theta_{Ybi}} + \sum_{i=1}^{n_x} \frac{\eta_{Pi}}{\eta_{Yi}}\right]}{[n_c(\text{bcoldu} - 1) + n_b(\text{bgirdu} - 1) + n_x(\text{bbradu} - 1)]}, \tag{84}$$

where bcoldu (= 4.0) is the bad value of column accumulated plastic hinge rotation ductility; bgirdu (= 6.0), bad value of girder accumulated plastic hinge rotation ductility; bbradu (= 4.0), bad value of brace accumulated plastic extension ductility; n_c, number of specified cross sections of columns (= 16 in the case of a four-story one-bay frame); n_b, number of specified cross sections of girders (= 12); n_x, number of bracing members (= 8); θ_{Pci}, column accumulated plastic hinge rotation corresponding to 16% exceedance probability; θ_{Yci}, column yield rotation (anti-symmetric double curvature deformation); θ_{Pbi}, girder accumulated plastic hinge rotation corresponding to 16% exceedance probability; θ_{Ybi}, girder yield rotation (anti-symmetric double curvature deformation); η_{Pi}, brace accumulated plastic extension corresponding to 16% exceedance probability; and η_{Yi}, brace yield extension.

Then, the dissatisfaction level of this accumulated plastic deformation ductility ratio is defined as follows:

$$D = \frac{\text{gplast} - P_r}{\text{gplast} - \text{bplast}} \tag{85}$$

where bplast (= 0.0) is the bad value of accumulated plastic deformation ductility ratio (this value 0.0 indicates completely elastic response under severe earthquakes) and gplast (= 0.2) is the good value of accumulated plastic deformation ductility ratio (this value depends strongly on a designer's subjectivity regarding the concept of safety).

This definition of dissatisfaction level for accumulated plastic deformation ductility ratio corresponds to the aim of accepted design philosophy. The parameter bplast = 0.0 means that it is unfavorable to resist severe earthquakes completely elastically. On the other hand, the parameter gplast depends on a designer's subjectivity. When a structural designer desires to design a building frame which needs a relatively larger safety factor, he or she may employ a relatively smaller value of gplast (Fig. 11a). Otherwise, he or she may employ a relatively larger value of gplast close to 1.0 (Fig. 11b).

5.8. *Design variables and optimal design problem*

While the moments of inertia and cross-sectional areas were taken as design variables in Sec. 3, three parameters $\bar{R}$, r, and ζ defined in Sec. 3.3 are employed as design variables in this section. The choice is influenced by the fact that since there are many members in a practical building frame, it is difficult from the computational point of view to employ moments of inertia and cross-sectional areas

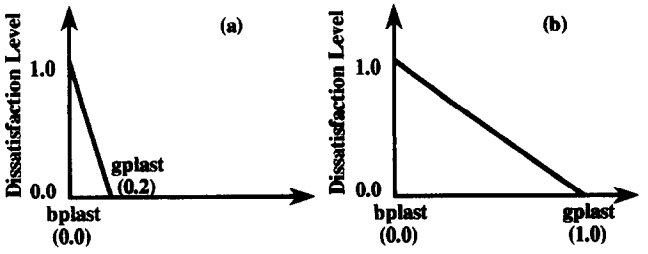

Fig. 11. Dissatisfaction level for accumulated plastic deformation ductility ratio.

of members as design variables even after reducing the number of design variables by grouping. Another reason results from the intention of the authors to try to incorporate the designer's experience and intuition into the design process as much as possible. Since the design variables $\bar{R}$, r, and $\bar{\zeta}$ have definite, mechanically meaningful characteristics described before, it is easy to reflect the designer's experience and intuition in terms of $\bar{R}$, r, and $\bar{\zeta}$.

It should be noted that only the dynamic stiffness design introduced in Sec. 4 is considered in this section. Therefore, once the three parameters $\bar{R}$, r, and $\bar{\zeta}$ are determined, the moments of inertia and plastic moments of girders and columns and the cross-sectional areas of bracing members are obtained from the dynamic stiffness design method presented in Sec. 4. One of the reasons to use the dynamic stiffness design method is to avoid the so-called whipping phenomenon which is difficult to control by imposing the design constraints employed in typical mathematical programming problems.

In this section, the following *min–max problem* is considered: Find the design variables $\bar{R}$, r, and $\bar{\zeta}$ which minimize the maximum dissatisfaction level, max D_i, under the condition that all the dissatisfaction levels of the constraints are smaller than 1.0. The values of D_i represent the dissatisfaction levels of the constraints and of the accumulated plastic deformation ductility ratio.

5.9. *Procedure for improving the dissatisfaction level*

The dissatisfaction level for each constraint and that for accumulated plastic deformation ductility ratio can be evaluated by carrying out response simulations for the three limit states. It should be noted that a series of time history analyses is performed both for 100 moderate earthquake ground motions and for 100 severe earthquake ground motions to obtain probabilistic distributions of peak responses. It is possible to regard the design constraints as the design objectives after all of the dissatisfaction levels associated with the design constraints are smaller than 1.0, i.e., a feasible design has been obtained. It may therefore be said that the problem stated in the previous section is a multi-objective optimal design problem. In this section the improvement procedure for dissatisfaction levels is explained.

Let p_k $(k = 1, \ldots, n)$ denote the dissatisfaction levels of the epsilon-active constraints (including accumulated plastic deformation ductility ratio). For simplicity of expression, the design parameters $\bar{R}$, r, and $\bar{\zeta}$ are denoted here by x_1, x_2, and x_3, respectively. The dissatisfaction level derivatives with respect to the design parameters can be evaluated by the following finite difference procedure

$$\frac{\partial p_k}{\partial x_1} = \frac{p_k(x_1 + \Delta x_1, x_2, x_3) - p_k(x_1, x_2, x_3)}{\Delta x_1} \tag{86a}$$

$$\frac{\partial p_k}{\partial x_2} = \frac{p_k(x_1, x_2 + \Delta x_2, x_3) - p_k(x_1, x_2, x_3)}{\Delta x_2} \tag{86b}$$

$$\frac{\partial p_k}{\partial x_3} = \frac{p_k(x_1, x_2, x_3 + \Delta x_3) - p_k(x_1, x_2, x_3)}{\Delta x_3}. \tag{86c}$$

For simplicity of expression, consider the case where there exist only two epsilon-active constraints. Let p_m and p_n denote the dissatisfaction levels of the epsilon-active constraints. Figure 12(a) shows the

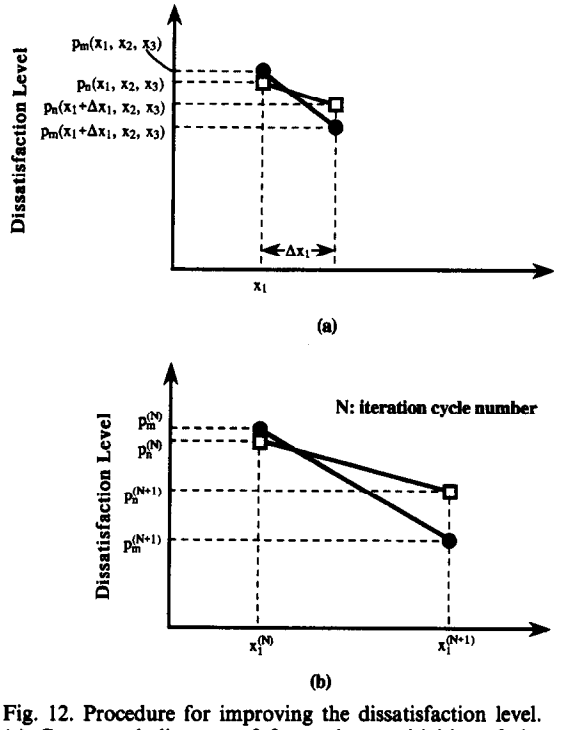

Fig. 12. Procedure for improving the dissatisfaction level. (a) Conceptual diagram of first-order sensitivities of the epsilon active dissatisfaction levels. (b) Typical example of the transition of the maximum dissatisfaction level.

conceptual diagram of the first-order sensitivities of the epsilon-active dissatisfaction levels and Fig. 12(b) illustrates a typical example of the transition of the maximum dissatisfaction level. Now the optimality criteria may be stated as follows:

(i) If $\partial p_m/\partial x_i$, $\partial p_n/\partial x_i$ have the same sign in either of $i = 1, 2, 3$, then we can improve the maximum dissatisfaction level.
(ii) If $\partial p_m/\partial x_i$, $\partial p_n/\partial x_i$ have the opposite sign for all x_is, then we have reached one of the optimum designs (Pareto optimal).

It is straightforward to extend these criteria to the case where several constraints are epsilon-active. Furthermore, it is of great importance to note that the optimal design described above can be interpreted as a special kind of Pareto optimal in the sense that only the epsilon-active constraints (also objectives in a feasible region) satisfy the requirement of Pareto optimal.

It is apparent that there exist many paths to one of the Pareto optimal solutions. The judgment should be made by each structural engineer as to which path to take. Some engineers may make a decision based on their experience and other engineers based on their intuition. Then, the proposed design method brings structural engineers useful information. If the maximum dissatisfaction level can be improved by $\bar{R}$, r, and $\tilde{\zeta}$, an engineer may adopt an improvement procedure based upon the following information: (i) The improvement by means of $\bar{R}$ implies design modification resulting in the change of story stiffness with the girder-to-column stiffness or strength ratio and the moment-resisting frame participation ratio in story shear forces almost constant. (ii) The improvement by means of r implies design modification resulting in the change of girder-to-column stiffness or strength ratio with each story stiffness and the moment-resisting frame participation ratio in story shear forces almost constant. (iii) The improvement by means of $\tilde{\zeta}$ implies design modification resulting in the change of moment-resisting frame participation ratio in story shear forces with each story stiffness and the girder-to-column stiffness or strength ratio almost constant. Thus, this design method provides the designer with mechanically meaningful information. For example, if an engineer makes an evaluation such that the present design has an undesirable girder-to-column stiffness or strength ratio, he or she may adopt an improvement via r. A similar procedure is applicable to the improvement via $\bar{R}$ or $\tilde{\zeta}$ when the present design has an undesirable story stiffness or an undesirable moment-resisting participation ratio in story shear forces.

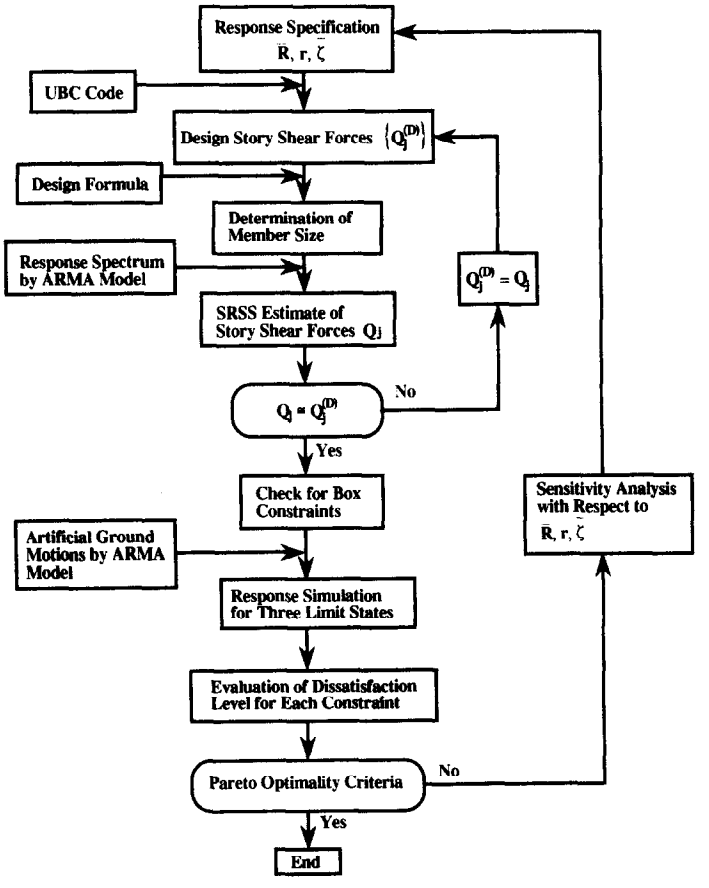

Fig. 13. Flow diagram for probabilistic multi-objective optimal design method.

It should be noted finally that it is guaranteed in this design algorithm that once a feasible design is obtained, which requires the maximum dissatisfaction level of the design constraints to be smaller than 1.0, each successive design is also feasible and has a lower maximum dissatisfaction level. The flow diagram of the probabilistic multi-objective optimal design method is shown in Fig. 13.

5.10. *Design examples*

Design example 1. Consider a four-story one-bay concentrically braced steel frame shown in Fig. 8. The span length and story height are $L = 15$ ft and $h_i = 10$ ft ($i = 1, \ldots, 4$). This frame is assumed to be one of many similar frames spaced at 20 ft centers in a three-dimensional structure. Applied gravity loads are shown in Fig. 8(a). The frame's geometry, masses and boundary conditions are fixed throughout the design process. Each frame is modeled as a two-dimensional structure with its masses lumped at the nodes. The first-story column bases are assumed to be fixed and torsional effects are ignored in the design.

Frame loads are composed of dead and live gravity loads plus lateral seismic loading (see Fig. 8). Wind, snow and vertical ground accelerations are neglected for simplicity. Nominal dead and live gravity loads are 80 and 40 psf, respectively, on all floors and the roof, and are modeled deterministically. For the limit state defined by gravity loads alone, loads consist of the structure's dead load plus the nominal live load. When an earthquake occurs, however, the nominal live load is multiplied by a reduction factor of 0.88 to approximate the mean lifetime value. In order to prevent bracing members from buckling under gravity loads, an initial tensile force of 11.25 kips has been introduced in every bracing member.

The design example corresponding to the design varaible grouping [case 1] is considered here. In utilizing the UBC code in the first iteration cycle, the following design conditions are adopted; seismic zone 4 (seismic zone factor $Z = 0.40$), site coefficients $S = 1.2$ (type S_2), importance factor $I = 1.0$, factor dependent on type of structural systems $R_W = 8.0$. An initial design is obtained by specifying the design parameters ($\bar{R} = 0.0015$ rad, $r = 0.7$, $\bar{\zeta} = 0.10$, $q_1 = 0.8$, $q_3 = 1.0$, $p_1 = 1.0$, $p_3 = 1.0$) for the mean plus one standard deviation acceleration response spectrum described in Sec. 2.1. The damping ratio in every mode is assumed to have a constant value of 0.03 in the dynamic stiffness design method. The mean plus one standard deviation acceleration response spectrum is adopted here because the design method developed in Secs 5.6–5.9 is based on a reliability concept and this mean plus one standard deviation acceleration response spectrum is consistent with this concept.

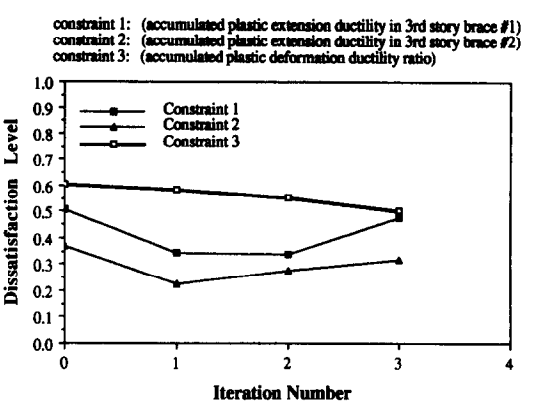

Fig. 14. Dissatisfaction level vs iteration number in multi-objective optimal design (design example 1: design variable grouping [case 1]).

Figure 14 shows dissatisfaction levels of constraints and accumulated plastic deformation ductility ratio for the initial design. The maximum dissatisfaction level is associated with the constraint on accumulated plastic extension ductility in the third story bracing member and with the accumulated plastic deformation ductility ratio. Table 2 presents the sensitivities of the dissatisfaction levels of epsilon-active constraints and the dissatisfaction level of accumulated plastic deformation ductility ratio with respect to design parameters evaluated at the initial design. It can be predicted from Table 2 that the reduction of the maximum dissatisfaction level will be successfully performed either by increasing the design parameter r or by decreasing $\bar{\zeta}$.

Figure 14 also illustrates the dissatisfaction levels vs iteration number. Improvement of dissatisfaction levels has been performed by reducing $\bar{\zeta}$ to 0.06 in the second iteration cycle. Then, further improvement has been made by increasing $\bar{R}$ to 0.00155 rad. After the third iteration, a solution to the min–max problem was obtained. It can be observed from Fig. 14 that improvement of the maximum dissatisfaction

Table 2. Sensitivity of dissatisfaction levels of epsilon-active constraints with respect to design parameters (design example 1: initial design)

Description	Dissatisfaction (D)	$\partial D/\partial x_1$	$\partial D/\partial x_2$	$\partial D/\partial x_3$
Accumulated plastic extension ductility (3rd story brace)	0.506	1180	-1.2	6.4
Accumulated plastic deformation ductility ratio	0.604	-770	-0.98	0.84

($x_1=\bar{R}$, $x_2=r$, $x_3=\bar{\zeta}$)

Table 3. Sensitivity of dissatisfaction levels of epsilon-active constraints with respect to design parameters (design example 1: optimal design)

Description	Dissatisfaction (D)	$\partial D/\partial x_1$	$\partial D/\partial x_2$	$\partial D/\partial x_3$
Accumulated plastic extension ductility (3rd story brace)	0.476	2800	-0.06*	-1.6
Accumulated plastic deformation ductility ratio	0.500	-1040	-0.58*	2.4

($x_1=\bar{R}$, $x_2=r$, $x_3=\bar{\zeta}$)

(* Although this sensitivity means that the maximum dissatisfaction level can be improved by increasing the parameter r, the increase of r does not necessarily improve it. This is because the moment of inertia of the second floor girder is close to the lower bound of the box constraint and further development of plastic deformation can not be expected.)

level associated with the constraint on accumulated plastic extension ductility in the third story bracing member cannot be performed without violating the requirement on accumulated plastic deformation ductility ratio at the final design.

Table 3 shows the sensitivities of the epsilon-active dissatisfaction levels with respect to design parameters evaluated at the final design. Although the sensitivity with respect to r means that the maximum dissatisfaction level can be improved by increasing the parameter r, the increase of r does not necessarily improve it. This is because the moment of inertia of the second floor girder is close to the lower bound of the box constraint and further development of plastic

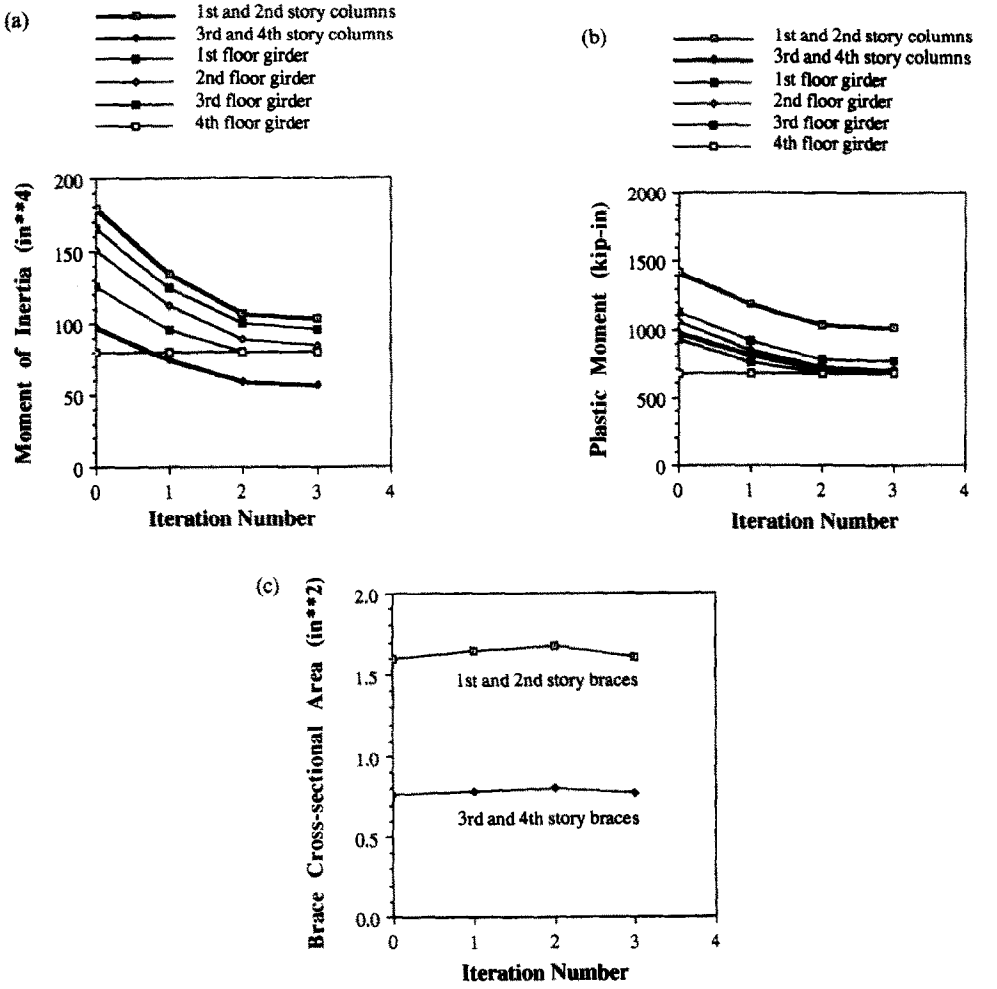

Fig. 15. (a) Moment of inertia vs iteration number (design example 1). (b) Plastic moment vs iteration number (design example 1). (c) Brace cross-sectional area vs iteration number (design example 1).

deformation can not be expected. Therefore the final design can be regarded as an optimal design. The accumulated plastic hinge rotation ductilities of the first, second, third, and fourth floor girders corresponding to 16% exceedance probability are (2.13, 2.96, 2.43, 0.0), respectively. In addition, the accumulated plastic extension ductilities of the first, second, third, and fourth story bracing members corresponding to 16% exceedance probability are (0.0, 0.0, 2.95, 1.70), respectively.

The moment of inertia vs iteration number and the plastic moment vs iteration number for the girders and columns are plotted in Figs 15(a), (b). The cross-sectional area vs iteration number for the bracing members is plotted in Fig. 15(c). It can be clearly observed from Figs 15(a)–(c) that the parameter $\bar{\zeta}$ controls the moment-resisting frame participation ratio just as the parameter $\bar{R}$ controls the story stiffness. The fundamental periods of the initial design and the optimal design are 0.322 and 0.329 sec, respectively.

Design example 2. Consider again the same model as shown in Fig. 8. In order to treat the case where brace slenderness ratio is relatively small, a frame corresponding to the case where there is a lateral-load resisting core in a five-bay frame in which the bays, except the core, sustain only gravity loads is considered. Gravity loads are identical to those of the previous example, but concentrated masses at the nodes are multiplied by a factor of five when considering motion in the horizontal direction.

The design example corresponding to the design variable grouping [case 1] is considered here again. An initial design is obtained by specifying the design parameters ($\bar{R} = 0.0015$ rad, $r = 0.7$, $\bar{\zeta} = 0.25$, $q_1 = 0.8$, $q_3 = 1.0$, $p_1 = 1.0$, $p_3 = 1.0$) for the mean plus one standard deviation acceleration response spectrum described in Sec. 2.1.

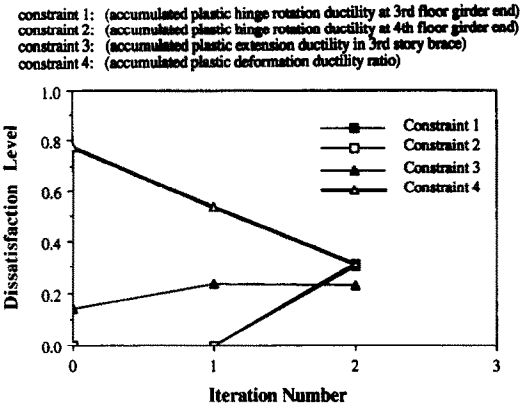

Fig. 16. Dissatisfaction level vs iteration number in multi-objective optimal design (design example 2: design variable grouping [case 1]).

Figure 16 shows dissatisfaction levels of constraints and accumulated plastic deformation ductility ratio for the initial design. The maximum dissatisfaction level is associated with the accumulated plastic deformation ductility ratio. Table 4 presents the sensitivities of the dissatisfaction level of accumulated plastic deformation ductility ratio with respect to design parameters evaluated at the initial design. It can be predicted from Table 4 that the reduction of the maximum dissatisfaction level will be successfully performed either by increasing the design parameter $\bar{R}$, by increasing r or by increasing $\bar{\zeta}$.

Table 4. Sensitivity of dissatisfaction levels of epsilon-active constraints with respect to design parameters (design example 2: initial design)

Description	Dissatisfaction (D)	$\partial D/\partial x_1$	$\partial D/\partial x_2$	$\partial D/\partial x_3$
Accumulated plastic deformation ductility ratio	0.778	-4.84	-0.68	-0.540

$(x_1=\bar{R},\ x_2=r,\ x_3=\bar{\zeta})$

Table 5. Sensitivity of dissatisfaction levels of epsilon-active constraints with respect to design parameters (design example 2: optimal design)

Description	Dissatisfaction (D)	$\partial D/\partial x_1$	$\partial D/\partial x_2$	$\partial D/\partial x_3$
Accumulated plastic hinge rotation ductility (3rd floor girder)	0.302	9152	6.04	4.12
Accumulated plastic hinge rotation ductility (4th floor girder)	0.310	9394	6.19	-5.64
Accumulated plastic extension ductility (3rd story brace)	0.231	-30.3	-2.10	-0.953
Accumulated plastic deformation ductility ratio	0.313	-6758	-2.72	-0.800

$(x_1=\bar{R},\ x_2=r,\ x_3=\bar{\zeta})$

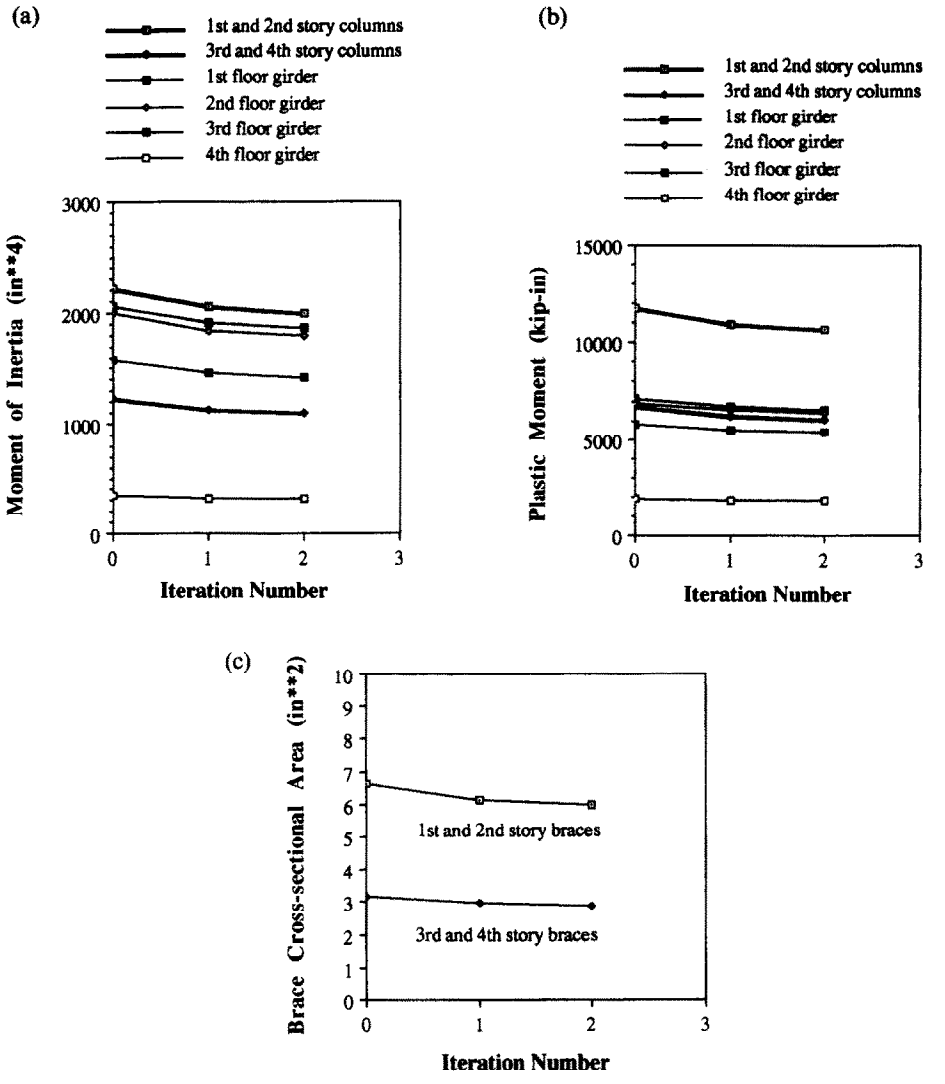

Fig. 17. (a) Moment of inertia vs iteration number (design example 2). (b) Plastic moment vs iteration number (design example 2). (c) Brace cross-sectional area vs iteration number (design example 2).

Figure 16 also illustrates the dissatisfaction levels vs iteration number. Improvement of the maximum dissatisfaction level has been made by increasing $\bar{R}$ to 0.001633 rad. After the second iteration, an approximate solution to the min–max problem was obtained. It can be observed from Fig. 16 that improvement of the maximum dissatisfaction level associated with the constraints on accumulated plastic extension ductility in the third story bracing member and on accumulated plastic hinge rotation ductility in the third and fourth floor girders cannot be obtained without violating the requirement on accumulated plastic deformation ductility ratio at the final design.

Table 5 shows the sensitivities of the epsilon-active dissatisfaction levels with respect to design parameters evaluated at the final design. It can be found from Table 5 that the final design satisfies the condition for optimality described in Sec. 5.9. Furthermore, the accumulated plastic hinge rotation ductilities of the first, second, third, and fourth floor girders corresponding to 16% exceedance probability are (0.0, 1.30, 4.60, 4.62), respectively. In addition, the accumulated plastic extension ductilities of the first, second, third, and fourth story bracing members corresponding to 16% exceedance probability are (1.06, 1.52, 2.46, 1.55), respectively.

The moment of inertia vs iteration number and the plastic moment vs iteration number for the girders and columns are plotted in Figs 17(a), (b). The cross-sectional area vs iteration number for the bracing members is plotted in Fig. 17(c). It can be observed from Figs 17(a)–(c) that the initial design adopted here is close to the optimal design from the standpoint of member size. This demonstrates that the dynamic stiffness design method can provide a fairly good initial design if the design parameters are appropriately chosen based upon designer's experience and/or some other information. Nevertheless the

dissatisfaction level of accumulated plastic deformation ductility ratio shows high sensitivity to a small change of member size. This is because a relatively small value of gplast has been adopted in this example. The fundamental periods of the initial design and the optimal design are 0.322 and 0.339 sec, respectively.

6. SUMMARY AND CONCLUSIONS

The objectives of this paper are (i) to present a simplified stiffness design method, called 'decomposed stiffness design method', for concentrically braced steel frames under seismic loading and (ii) to propose a probabilistic multi-objective optimal design method aimed at finding a satisfactory design with the least dissatisfaction level under multiple design conditions.

A design process has been described, which first utilizes a stiffness-oriented static design method to determine the member size of a frame showing the specified response to static lateral loading. The main feature of this design method is to deal with the moment-resisting frame and the bracing system independently. This initial design is then examined by a dynamic design procedure which employs a dynamic ARMA model as a simulator for design earthquakes and utilizes the SRSS procedure. A probabilistic multi-objective optimal design method for concentrically braced steel frames is then introduced to formulate a general seismic-resistant design problem taking into account the probabilistic response characteristics due to uncertainty of design earthquakes. Two design examples were presented to demonstrate the validity of this design method.

The characteristic features of this investigation may be summarized as follows:

1. The practicality and reliability of this multi-objective optimal design method are guaranteed because all the constraints for three limit states, which are defined based upon the accepted design philosophy, are taken into account.

2. It is guaranteed in this multi-objective optimization algorithm that once a feasible design is obtained, which requires a dissatisfaction level for each design constraint to be smaller than 1.0, each successive design is also feasible and has a lower maximum dissatisfaction level. Therefore the designer can stop at any stage within the feasible region, depending upon the computational resources available for the design.

3. Probabilistic evaluation of the seismic response of a concentrically braced steel frame is reliable because of the use of a dynamic ARMA model as a simulator of design earthquakes and the use of inelastic time history analysis within the design process itself rather than as a check at the final stage.

4. The accumulated plastic deformation ductility ratio introduced in this paper can better reflect the aim of the accepted design philosophy than the minimum volume criterion.

5. The present comprehensive design procedure includes three design phases, i.e., the stiffness design method for equivalent static lateral loading, the dynamic design method using the design response spectra constructed from a set of artificial earthquakes generated by a dynamic ARMA model, and the probabilistic multi-objective optimal design method. Therefore, this design procedure can be utilized not only as a tool for providing a good initial design following usual structural design practice but also as an efficient structural design algorithm.

6. The design procedure has the flexibility to be able to incorporate other types of design constraints and design objectives.

7. The technique of handling of design constraints can reflect a structural designer's objectives more appropriately than the usual deterministic technique adopting rigid constraint boundaries. Moreover, a multi-objective optimization problem can be formulated according to the structural designer's intention. This formulation regarding the design constraints as the design objectives is a new type of formulation of multi-objective optimal design problems.

8. The present stiffness-oriented design formula employs mechanically meaningful parameters as principal design parameters, i.e., story stiffness, girder-to-column stiffness ratio and ratio of moment-resisting frame stiffness to the total story stiffness (frame participation ratio). Therefore, it is relatively easy to reflect the designer's intuition and/or experience in using this design formula. This facilitates the development of an interactive environment between the designer and a computer.

It may be said that the proposed probabilistic multi-objective optimal design method can play an important role in providing the designer with an interactive decision making environment. Such an environment cannot be provided by a blackbox including only a mathematical programming algorithm. It should be remarked finally that this multi-objective optimal design method can readily be extended to the case where the site under consideration is faced with several different active faults and it is possible to regard all or some of them as the design earthquakes. In this case, it seems reasonable to generate a population of artificial ground motions for each design earthquake by means of this dynamic ARMA model and to deal with the constraints for each design earthquake as independent design constraints. Then the dissatisfaction levels for each design earthquake could be evaluated in a common graph.

Acknowledgements—This research work was carried out during the first author's stay at the University of California at Berkeley during the academic year 1989–1990 as a visiting scholar. The assistance of the Kajima Foundation (Japan) to the first author is gratefully acknowledged. The first author would like to express his appreciation to Professors Tsuneyoshi Nakamura and Koji Uetani of Kyoto University for providing the opportunity to work at the University of California at Berkeley.

REFERENCES

1. K. S. Pister, Optimal design of structures under dynamic loading. In *Optimization of Distributed Parameter Structures* (Edited by E. J. Haug and J. Cea) Vol. I, pp. 569–585. Sijthoff & Noordhoff, Alphen aan den Rijn (1980).
2. J. C. Anderson and V. V. Bertero, Uncertainties in establishing design earthquakes. *J. Struct. Engng, ASCE* **113,** 1709–1724 (1987).
3. J. C. Anderson, Seismic behavior of K-braced framing systems. *J. Struct. Div., ASCE* **101,** 2147–2159 (1975).
4. S. A. Mahin and V. V. Bertero, Prediction of nonlinear seismic building behavior. *J. Technical Council, ASCE* **104,** 21–37 (1978).
5. J. P. Lin and S. A. Mahin, Effect of inelastic behavior on the analysis and design of earthquake resistant structures. Report No. EERC 85-08, Earthquake Engineering Research Center, University of California, Berkeley, CA (1985).
6. L. J. Branstetter, G. D. Jeong, J. T. P. Yao, Y. K. Wen and Y. K. Lin, Mathematical modelling of structural behavior during earthquakes. *Probabilistic Engng Mech.* **3,** 130–145 (1988).
7. O. E. Lev, *Structural Optimization: Recent Developments and Applications.* ASCE (1981).
8. Tsuneyoshi Nakamura and Y. Takenaka, Optimum design of multistory multispan frames for prescribed elastic compliance. *J. Struct. Mech.* **11,** 271–295 (1983).
9. Tsuneyoshi Nakamura and I. Takewaki, Ductility design via optimum design of nonlinear elastic frames. *J. Struct. Engng. ASCE* **115,** 608–625 (1989).
10. Tsuneyoshi Nakamura and M. Ohsaki, Sequential generator of earthquake-response constrained trusses for design strain ranges. *Comput. Struct.* **33,** 1403–1416 (1989).
11. K. Furukawa and H. Furuta, A new formulation of optimum aseismic design using fuzzy mathematical programming. *Proc. of 8th World Conf. on Earthquake Engng* **V,** 443–450. San Francisco, CA (1984).
12. G.-Y. Wang and W.-Q. Wang, Fuzzy optimum design of aseismic structures. *Earthquake Engng Struct. Dyn.* **13,** 827–837 (1985).
13. G.-Y. Wang and W.-Q. Wang, Fuzzy optimum design of structures. *Engng Optimization* **8,** 291–300 (1985).
14. I. Takewaki and Tsuneyoshi Nakamura, Fuzzy optimum design of shear buildings. *Proc. Ist Japan Conf. on Struct. Safety and Reliability,* pp. 459–464 (1987) (in Japanese).
15. S. S. Rao, Multi-objective optimization of fuzzy structural systems. *Int. J. Numer. Meth. Engng* **24,** 1157–1171 (1987).
16. M. A. Bhatti and K. S. Pister, A dual criteria approach for optimal design of earthquake-resistant structural systems. *Earthquake Engng Struct. Dyn.* **9,** 557–572 (1981).
17. R. J. Balling, K. S. Pister and V. Ciampi, Optimal seismic-resistant design of a planar steel frame. *Earthquake Engng Struct. Dyn.* **11,** 541–556 (1983).
18. M. A. Austin and K. S. Pister, Design of seismic-resistant friction-braced frames. *J. Struct. Engng. ASCE* **111,** 2751–2769 (1985).
19. M. A. Austin, K. S. Pister and S. A. Mahin, A methodology for the computer-aided design of seismic-resistant steel structures. Report No. EERC 85-13, Earthquake Engineering Research Center, University of California, Berkeley, CA (1985).
20. M. A. Austin, K. S. Pister and S. A. Mahin, Probabilistic design of earthquake-resistant structures. *J. Struct. Engng, ASCE* **113,** 1642–1659 (1987).
21. M. A. Austin, K. S. Pister and S. A. Mahin, Probabilistic design of moment-resistant frames under seismic loading. *J. Struct. Engng, ASCE* **113,** 1660–1677 (1987).
22. I. F. Khatib, Seismic behavior of concentrically braced steel frames. Ph.D. dissertation, Structural Engineering, Mechanics and Materials, Department of Civil Engineering, University of California, Berkeley, CA (1987).
23. I. Takewaki, J. P. Conte, S. A. Mahin and K. S. Pister, A unified earthquake-resistant design method for steel frames using ARMA models. Report No. EERC 90-07, Earthquake Engineering Research Center, University of California, Berkeley, CA (1990).
24. I. Takewaki, J. P. Conte, S. A. Mahin and K. S. Pister, A probabilistic earthquake resistant design method for braced steel frames using ARMA models. Report No. UCB/SEMM 90-08, Department of Civil Engineering, University of California, Berkeley, CA (1990).
25. Recommended Lateral Force Requirements and Commentary, Seismology Committee, Structural Engineers Association of California, San Francisco, CA (1975).
26. R. V. Whitman and C. A. Cornell, Design. In *Seismic Risk and Engineering Decision* (Edited by C. Lomnitz and E. Rosenblueth). Elsevier, New York (1976).
27. R. F. Nau, R. M. Oliver and K. S. Pister, Simulating and analyzing artificial non-stationary earthquake ground motions. *Bull. Seismological Soc. Am.* **72,** 625–636 (1982).
28. J. P. Conte, ARMA models for earthquake excitation and structural response simulation. Report No. CE299, Department of Civil Engineering, University of California, Berkeley, CA (1988).
29. J. P. Conte, Influence of the earthquake ground motion process and structural properties on response characteristics of simple structures. Ph.D. dissertation, Department of Civil Engineering, University of California, Berkeley, CA (1990).
30. J. P. Conte, K. S. Pister and S. A. Mahin, Variability of structural response parameters within an earthquake. *Proc. of Fourth U.S. National Conf. on Earthquake Engng.* Palm Springs, CA (1990).
31. N. W. Polhemus and A. S. Cakmak, Simulation of earthquake ground motions using autoregressive moving average (ARMA) models. *Earthquake Engng Struct. Dyn.* **9,** 343–354 (1981).
32. M. K. Chang, J. W. Kwiakowski, R. F. Nau, R. M. Oliver and K. S. Pister, ARMA models for earthquake ground motions. *Earthquake Engng Struct. Dyn.* **10,** 651–662 (1982).
33. A. S. Cakmak, R. L. Sherif and G. Ellis, Modelling earthquake ground motions in California using parametric time series methods. *Soil Dyn. Earthquake Engng* **4,** 124–131 (1985).
34. F. Kozin, Autoregressive moving average models of earthquake records. *Probabilistic Engng Mech.* **3,** 58–63 (1988).
35. G. R. Saragoni and G. C. Hart, Nonstationary analysis and simulation of earthquake ground motions. Report No. UCLA-ENG-7238, Earthquake Engineering and Structures Laboratory, University of California, Los Angeles, CA (1972).
36. N. D. Walker, Automated design of earthquake resistant multistory steel building frames. Report No. EERC 77-12, Earthquake Engineering Research Center, University of California, Berkeley, CA (1977).
37. Uniform Building Code, International Conference of Building Officials, Whittier, CA (1988).
38. Tsuneyoshi Nakamura and I. Kosaka, Strain-controlled design of plane elastic building frames subjected to horizontal loads. *J. Struct. and Construction Engng, Trans AIJ* **363,** 1–11 (1986) (in Japanese).
39. Tsuneyoshi Nakamura and Lin Pang-shian, Design of beams for specified fundamental natural period and mode. *J. Struct. Engng,* Architectural Institute of Japan **34B,** 95–104 (1988) (in Japanese).

40. A. Der Kiureghian, A response spectrum method for random vibrations. Report No. EERC 80-15, Earthquake Engineering Research Center, University of California, Berkeley, CA (1980).
41. A. E. Kanaan and G. H. Powell, A general purpose computer program for dynamic analysis of inelastic plane structures–DRAIN-2D. A computer program distributed by National Information Service for Earthquake Engineering, Berkeley, CA (1973).
42. American Institute of Steel Construction, *Manual of Steel Construction*, seventh edition (1973).
43. W. T. Nye, DELIGHT: an interactive system for optimization-based engineering design. Report No. ERL M83-33, University of California, Berkeley, CA (1983).
44. W. T. Nye and A. L. Tits, An application-oriented, optimization-based methodology for interactive design of engineering systems. *Int. J. Control* **43**, 1693–1721 (1986).
45. W.-Y. Ng, Interactive multi-objective programming as a framework for computer-aided control system design, Vol. 132, *Lecture Notes in Control and Information Sciences*. Springer (1989).